GT2004-53758

BOUNDARY LAYER SUCTION VIA A SLOT IN A TRANSONIC COMPRESSOR - NUMERICAL PARAMETER STUDY AND FIRST EXPERIMENTS

K. Hubrich, A. Bölcs, P. Ott
Swiss Federal Institute of Technology
EPFL – ISE - LTT
1015 Lausanne, Switzerland
klaus.hubrich@epfl.ch

ABSTRACT

In the present paper a numerical and experimental study aiming at the enhancement of the working range of a transonic compressor via boundary layer suction (BLS) is presented. The main objective of the investigation is to study the influence of BLS on the interference between shock wave and boundary layer and to identify the possible benefit of BLS on the compressor working characteristics. An extensive numerical study has been carried out for the DATUM blade and for 2 different suction location configurations for one speed line and varying back-pressure levels, ranging from choked conditions to stall. It was found that the working range of the transonic compressor with a nominal inlet Mach number of 1.2 and a nominal pre-shock Mach number of 1.35 could be increased by sucking 2% of flow on the SS away, in such a way that the maximum pressure ratio and maximum diffusion could both be increased by 10%, when compared to the DATUM case. For smaller pressure ratios with respect to the design pressure ratio, the BLS is located in a supersonic flow region and thus creates additional losses due to a more divergent flow channel, which additionally accelerates the flow and results in a higher pre-shock Mach number creating higher losses.

First measurements carried out in LTTs annular cascade, do show reasonable agreement with the computations in terms of inlet Mach number, flow angle, main shock location and stall limit. The most pronounced difference between measurements and computations is the occurrence of a terminal normal channel shock behind a bowed detached shock wave and a separation on the SS of the blade, which were both not predicted by the CFD.

INTRODUCTION

The stage pressure ratio of jet-engine and gas-turbine compressors always tends to be increased in order to diminish the number of stages and thus the overall size and weight of such an apparatus. Transonic compressor stages are especially well suited for this purpose due to their high pressure-ratio, nowadays of up to 2 and higher. One of the main limiting factors for the transonic compressors is that the boundary layer usually separates when the pre-shock Mach number exceeds the value of 1.3, and that the pressure losses over a normal shock dramatically increase with high pre-shock Mach numbers. For example the pressure loss across a normal shock with a pre-shock Mach number of 1.5 becomes 10% and increases to 20% for a pre-shock Mach number of 1.73 (Bölcs 1993). One additional restriction for the application of transonic compressors with high pre-shock Mach numbers is the unique incidence conditions (Bölcs and Suter 1986), which means that for an attached shock wave only one single inlet Mach number is possible with one specific inlet flow angle regardless of the backpressure value. So the working range of a transonic compressor with relative supersonic inlet flow is very limited in terms of mass flow variations. This restriction means, that the mass flow for the stall limit is very close to the choked mass flow. As the efficiency at off-design operation of a gas turbine should still be elevated, a new approach is needed for overcoming this restriction in working range for the compressor.

One very promising method to overcome this restriction is boundary layer suction (BLS). Kerrebrock et al. (1997, Merchant 1999) report computations and designs with stage pressure ratios of up to 3.5 with a BLS mass flow of 3% in the rotor and 3% in the adjacent stator. A compressor pressure ratio of 30 would be attained with this design philosophy within 3 stages (Kerrebrock et al. 1998, Lord et al. 2000). Dang et al. (2003) proposed a 3D viscous inverse design method for designing transonic compressor rotors. It was numerically shown, that BLS was able to keep the shock inside the passage for higher backpressure values, and thus to enhance the working range of the compressor.

The objective of the current investigation is to study the influence of BLS on the rotor working-characteristic for one speed line from choked to stalled condition in terms of efficiency, pressure ratio, diffusion factor and mass flow. For this purpose a transonic rotor was designed with a design total

pressure ratio of 2 and an unusual high thickness in order to provide enough space for a cavity, through which the BLS mass flow could be dumped away. For studying the flow field in the compressor and especially the shock boundary layer interaction (SBLI) a numerical parameter study is performed where for the DATUM blade computations with 8 different backpressure levels have been carried out. Additionally two configurations with different BLS locations were numerically studied (44% and 53% of axial chord). The suction mass flow was kept constant at 2% of the design mass flow. The DATUM rotor was then manufactured and tested in LTTs annular cascade with an inlet Mach number of 1.12 and an inlet angle of 67 degree. The isentropic surface Mach number is compared to the predicted one. It is expected to identify via the numerical study the influence of BLS on the compressor characteristic and to verify experimentally for the DATUM blade if the prediction of the isentropic surface Mach number evolution would be correct.

NOMENCLATURE&ABREVIATIONS

BL	Boundary Layer
BLS	Boundary Layer Suction
D	Diffusion Factor
E	Work
$\dot{m}$	Mass flow rate
M	Mach Number
p	Pressure
PS	Pressure Side
s'	Blade Length
SBLI	Shock Boundary Layer Interaction
SS	Suction Side
t'	Blade Spacing
T	Temperature
Δ	Difference
$\prod$	Total Pressure Ratio pt2/pt1 in % of total design pressure ratio

Subscripts

isen	Isentropic Conditions
suction	Suction condition
s	Static Conditions
t	Total Conditions
u	Circumferential Component
1, 2	Inlet, Outlet

Chord Length [mm]	110
Axial Chord [mm]	65
Maximum Thickness [%]	6
Maximum Thickness [mm]	6.6
Inner Diameter [mm]	320
Outer Diameter [mm]	400
Maximum Mass Flow [kg/s]	10
Maximum Inlet Flow Angle [degree]	68
Maximum Pressure Ratio	4
Maximum Inlet Mach Number	1.5

table 1: Limiting geometrical conditions for the cascade with boundary layer suction

TRANSONIC ROTOR

For the present study a suitable transonic rotor was designed, which had to meet several restricting factors, imposed by LTTs annular cascade and its air supply (table 1). The length of the blade is limited to the length of the axial length of the measurement section. The thickness is a function of the length. The mass flow rate, the maximum inlet angle and the maximum inlet Mach number are limited by the main air supply of the test-rig and the geometry of the annular cascades pre-swirl vane. The result is a blade with an unusual high thickness for a transonic compressor rotor with an inlet Mach number of 1.2 and is shown in figure 1.
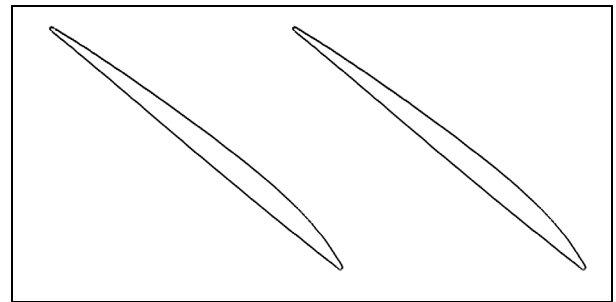

figure 1: Geometry of Transonic Rotor with 6% maximum thickness

COMPUTATIONAL METHOD&GRID

A modified version of MULTIP99 (J. Denton), which allows the extraction of mass flow on prescribed locations via a pressure outlet, was used to simulate the 3D flow in the rotor. Following the solver description of Chaluvadi et al 2003 and Denton and Xu 2002, MULTIP99 solves the three-dimensional modified Reynolds averaged Navier-Stokes equations on a structured, non-adaptive mesh. The equations of motion are discretised to second order accuracy and integrated forward in time. A mixing length model with wall function is used for modelling the turbulence in the flow. For the steady state calculations, a full multi-grid method and local time stepping are used to accelerate the convergence. The solver proved to be of same accuracy as other NS-solvers, as found by Gregory-Smith and Crossland, 2001.

The grid used has 37x157x37 cells, where a higher cell number (49x339x39) was tested but did not show enough differences to justify its use. A meridional view of the grid is shown in figure 2, the LE details in figure 3, and the TE details in figure 4. Convergence is typically attained when the averaged percentage change in the meridional velocity per time step is smaller than 0.2% for the DATUM cases. For the near stall cases this criterion was relaxed to a value of 0.5%, which is the initial criteria proposed by the author of the program (Denton 1999). This criterion implied at the present computational campaign a mass flow error over the computational domain in axial direction smaller than 1% of inlet mass flow.

Total pressure and temperature are mass averaged, the static pressure is area averaged. The isentropic efficiency is determined using the averaged total pressure and temperature values at inlet and outlet. In the case of BLS first an intermediate isentropic efficiency is determined with the mass

averaged data. With these data the isentropic outlet temperature is determined, which can be used in the following equation:

$$\eta_{isen} = \frac{E_{isen}}{E_{real}} = \frac{\dot{m} \cdot (T_{t2-isen} - T_{t1}) - \Delta\dot{m}_{suction} \cdot T_{t2-isen}}{\dot{m} \cdot (T_{t2} - T_{t1}) - \Delta\dot{m}_{suction} \cdot T_{t2}} \quad \text{eq. (1)}$$

For a suction mass flow amount of 2% for efficiencies in the range of 90% an efficiency penalty of 1% is obtained due to the suction. The efficiency determination considers neither the power needed to pump the fluid away nor a potential use of the suction mass flow as for example as cooling fluid.
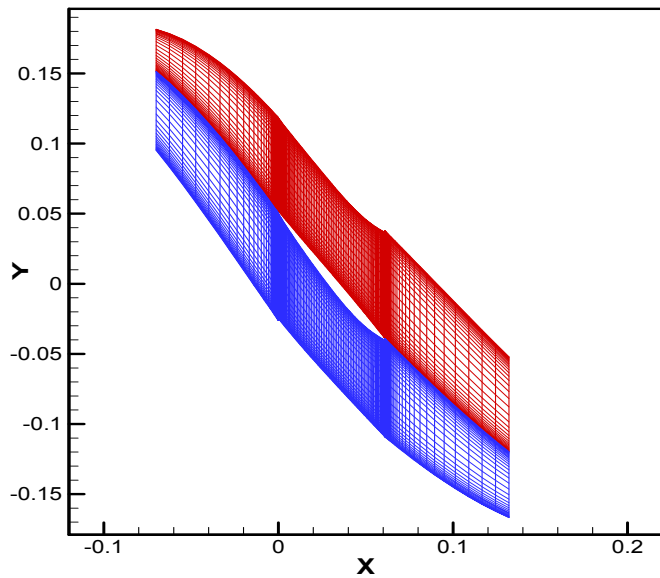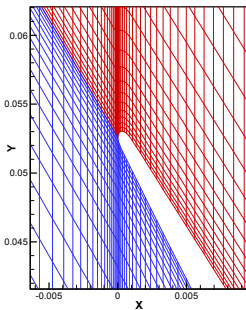

figure 2: Grid at mid-span of the blade

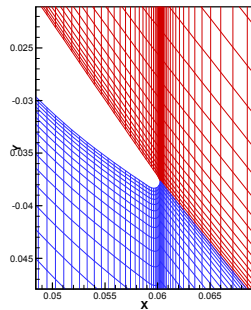**figure 3: Grid at LE of blade at midspan.**

figure 4: Grid at TE of blade at midspan

EXPERIMENTAL SET-UP

An annular cascade test-rig with a maximum inlet Mach number of up to 1.6 is utilized for aerodynamic measurements of the DATUM rotor. The main characteristics of the test rig are shown in table 2.

The main advantage of the annular cascade is that the air is pre-swirled by vanes and that the rotor remains fix. The same relative velocity as in a rotating rotor can be generated, but with a non-moving cascade. So it is without difficulty possible to connect pressure tap tubing for surface pressure measurements to the blade and to measure the static surface pressure on the blade for a supersonic inflow rotor. The working principle is shown in figure 5. The air is continuously delivered by a compressor (max. 2.5MWe) and enters the pre-swirl vanes at subsonic conditions. Here, the flow-angle can be set by varying the pitch-angle of the pre-swirl vanes. The subsequent radial-axial nozzle accelerates the flow to up to Mach numbers of 1.6 at the inlet of the measuring cascades. The truly attainable values do depend on the tested cascade's geometry.

Maximum inlet Mach number	1.6
Maximum Inlet Angle [degree]	70
Maximum Mass flow [kg/s]	10
Maximum Inlet Pressure [bar]	4
Maximum Power for Main Flow [MW]	2.5
Maximum Power for BL Suction [MW]	0.7

table 2: Test-rig characteristics

A more complete sketch of the test-rig is shown in figure 6, where it can be seen, that two settling chambers are used with each one having a set of pre-swirl vanes allowing to adjust more accurately over the span the inlet flow to the measurement section. In the sketch it is shown, that boundary layer suction on the channel walls up- and downstream the cascade is used to obtain a cleaner flow at the inlet and no stall at the outlet of the test-section. The recent modifications by Rottmeier (2003) simplified, among other improvements, the set-up of the flow conditions considerably due to an improved accuracy of the pre-swirl vane guidance mechanism.
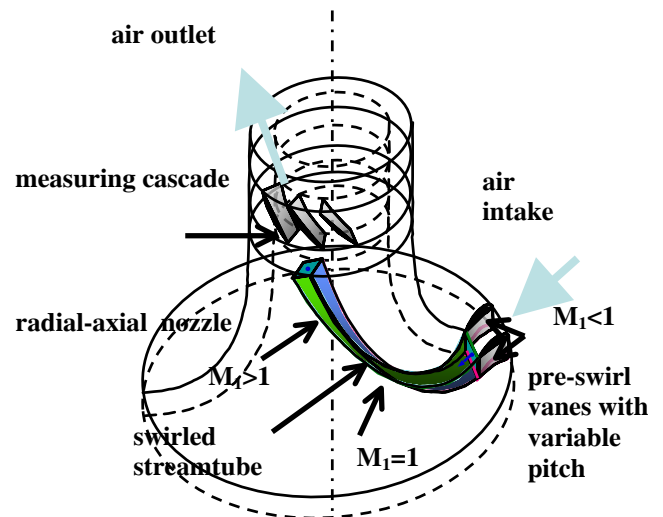

figure 5: Working principle of annular cascade

The static pressure taps are connected to a digital sensor array DSA 3017 from Scanivalve Corp. Each of the 6 used modules incorporates 16 temperature compensated piezoresistive pressure sensors and is connected via a TCP/IP connection to the PC. The accuracy is 0.05% of full scale, which translates to an accuracy of 100Pa or 1mbar. The inlet flow conditions are determined using an aerodynamic five-hole

pressure probe, which is as well connected to one DSA module and placed at approximately 0.6 chords upstream of the LE of the blade. The pressure probe can be traversed in radial direction and as the cascade can be rotated via a stepping motor in tangential direction the inlet Mach number is determined over a passage. The 5-hole aerodynamic pressure probe was calibrated in LTT's Laval nozzle to Mach numbers of up to 1.4 and flow angles of $\pm20^{o}$ for pitch and yaw angle. The stagnation temperature is measured using a temperature probe (K-type) in the settling chamber. The inlet Mach number is calculated via the isentropic relationship between stagnation and static pressure; both values are provided by the 5-hole aerodynamic probe.
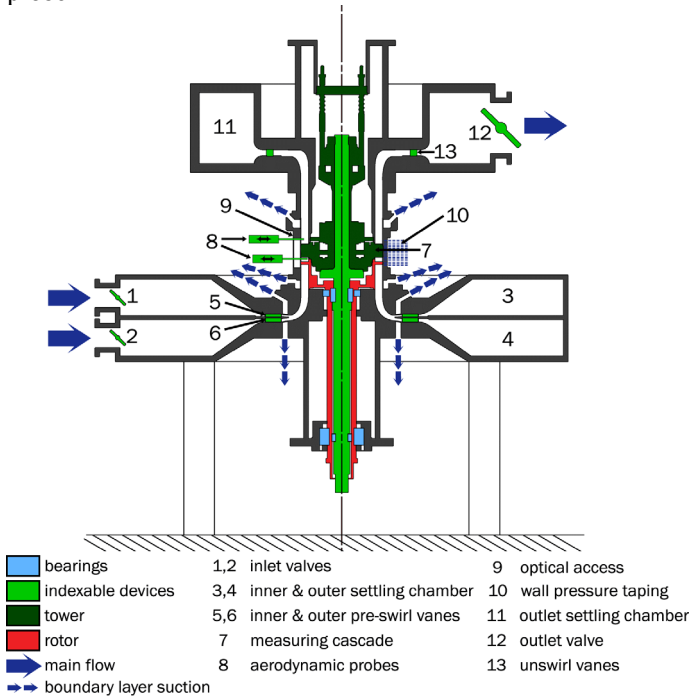

bearings	1,2	inlet valves	9 optical access
indexable devices	3,4	inner & outer settling chamber	10 wall pressure taping
tower	5,6	inner & outer pre-swirl vanes	11 outlet settling chamber
rotor	7	measuring cascade	12 outlet valve
main flow	8	aerodynamic probes	13 unswirl vanes
boundary layer suction			

figure 6: Sketch of the annular cascade installation (Rottmeier 2003)

NUMERICAL RESULTS

The results of the 3D computations are shown for the mid-span section in terms of the isentropic surface Mach number and subsequently as 2D Mach number contour plots.

In figure 7 the isentropic surface Mach number evolution is shown for the design pressure ratio of the DATUM blade and the two suction configurations with 2% suction mass flow. The inlet and outlet Mach numbers are similar for all three cases, which leads to a similar pressure rise for each configuration since the same inlet and exit boundary conditions (p_{t1}, T_{t1}, p_{s2}) are used. As the shock on the SS is located more downstream for both suction cases the shock Mach number is higher with respect to the DATUM configuration. The two distinct peaks over the suction locations are created by the suction itself. A smaller pressure value is experienced by the flow in this region, leading to a higher isentropic surface Mach number. Due to the suction the pressure and the flow angle is locally changed. These peaks are clearly connected to the suction and will be addressed in the next paragraph. An additional feature present in all Mach number graphs is the local increase of the Mach

number just in front of the LE of the blade, which is generated by the acceleration of the flow on SS of the neighbouring blade. The configuration with the suction at 44% ('suction 2') shows a distinct Mach number peak on the PS at 25%, which indicates the presence of a normal passage shock.

In figure 8 the isentropic surface Mach number evolution is shown for 114% of design pressure ratio. This is the highest pressure-ratio for which the DATUM case computation gave a converged result, so it is assumed that the flow stalls, slightly above this backpressure for the DATUM rotor. For both suction configurations the inlet Mach number remains constant at the design level and the shock position is identical for both suction configurations.
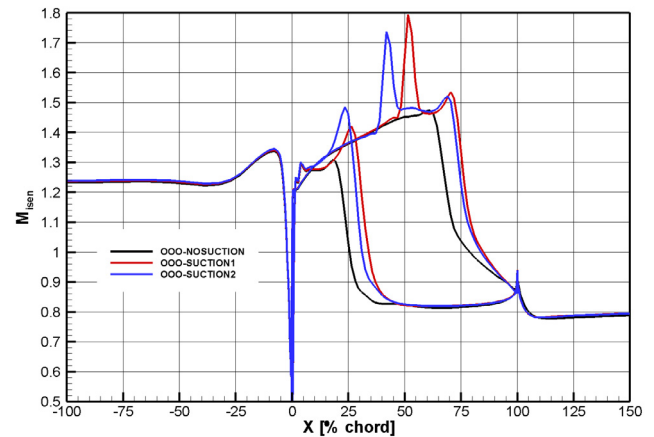

figure 7: Isentropic surface Mach number for $\prod=100\%$

The DATUM rotor shows no shock on the PS, which indicates the presence of a single shock wave, which is a detached bowed shock wave, leading to a smaller inlet Mach number. The shock is located at 30% chord. Despite the smaller inlet Mach number of the DATUM configuration the Mach number on the SS is higher for this configuration with respect to the suction configurations. This indicates an increase in flow angle at inlet and yields to a high acceleration around the LE of the blade. The outlet Mach number is smaller in comparison to the design configuration.
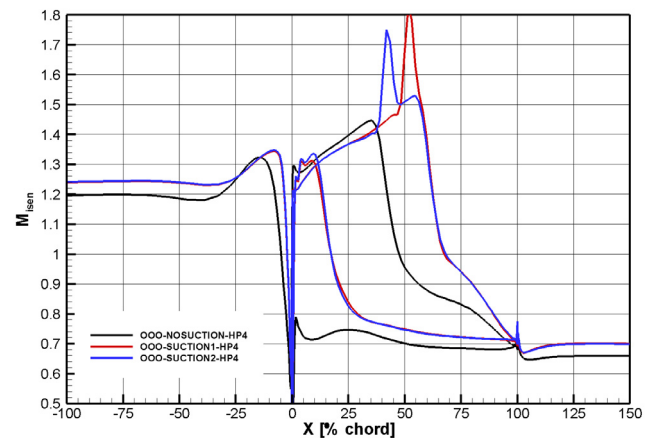

figure 8: Isentropic surface Mach number for $\prod=114\%$

In figure 9 the isentropic surface Mach number evolution is shown for the highest pressure-ratio, for which converged

results were only obtained for the cases with BLS. These two suction cases do show a smaller inlet Mach number as in the previous cases, which is now equivalent to the inlet Mach number of the DATUM rotor at ∏=114%. Here, both suction cases do show a very sharp shock position for a shock Mach number of 1.46 and a post-shock Mach number of 0.8. This would mean, that no separation occurs for this configuration. The Mach number evolution shows that no passage shock is present, only a detached bow shock wave is present indicating that the flow is at the verge to stall.
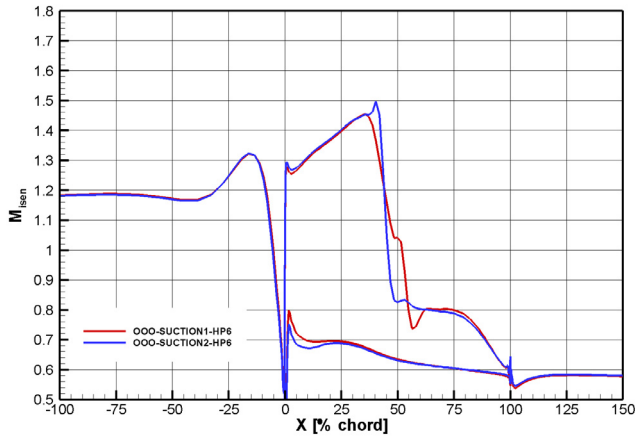
figure 9: Isentropic surface Mach number for ∏=123%

In figure 10 the 2D Mach number contours at mid-span are shown for the DATUM case at design pressure ratio. Here the assumed passage shock is present. The BL thickens on the SS due to the interaction with the shock and the SS curvature at the TE, but it can be seen, that the BL thickens as well on the PS, due to the passage shock. In front of the LE a detached bow shock wave is present, which rejoins the flow in the passage and reaccelerates to supersonic conditions. This subsonic area around the LE is created by the LE thickness of the blade and is typical for the flow in this rotor. In figure 11 the isentropic Mach number contour plot for the DATUM rotor at the stall limit is shown. Here the shock forms as a completely detached bow shock wave. At the LE a high acceleration peak can be detected on the SS, which is created by the higher inlet flow angle due to the detached bow shock wave.

In figure 12 the Mach number contours for the rotor with suction at 53% of chord are shown for the design pressure ratio. The suction location is stylized by a small black box. It can be spotted, that the BL decreases in thickness already in front of the suction. This is created by the additional acceleration of the flow, especially the BL due to the BLS. The BL is extremely thin up to the shock location, where it thickens considerably. Due to the change of flow direction over the suction location the flow accelerates additionally via a Prandtl-Meyer expansion wave. As behind the suction the flow has to follow the SS, a recompression occurs, which redirects the flow to the SS direction. The most remarkable feature of this configuration is that the expansion, which is created by the suction, interacts with the passage shock. This system of expansion and recompression is responsible for the Mach number peaks, which were already observed in the 1D surface Mach number evolution. The pre-shock Mach number of the shock on the PS is higher than the DATUM configuration making the post-

shock BL thicker. In figure 13 the Mach number contours are shown for the 53% suction case for a pressure ratio of 114% of design pressure ratio. The main difference to the DATUM case is that the shock remains in the passage and that the flow pattern looks similar to the one obtained for the DATUM case at design conditions. The shock BL interference zone shows a very thin BL that only thickens close to the TE.
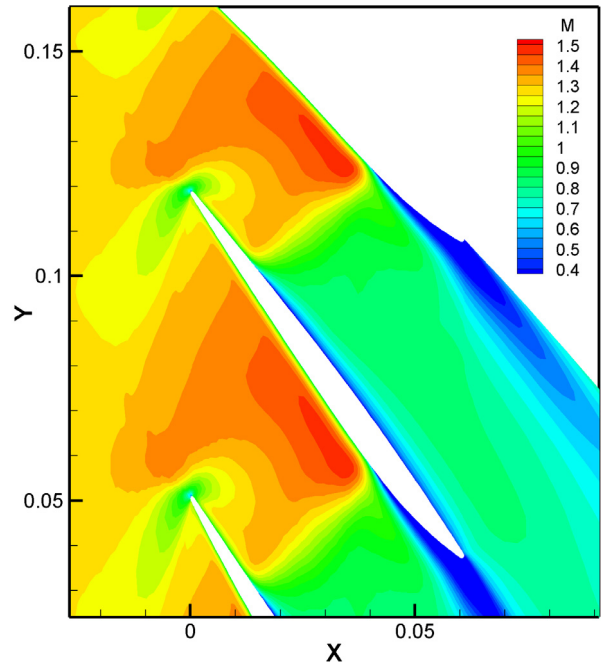

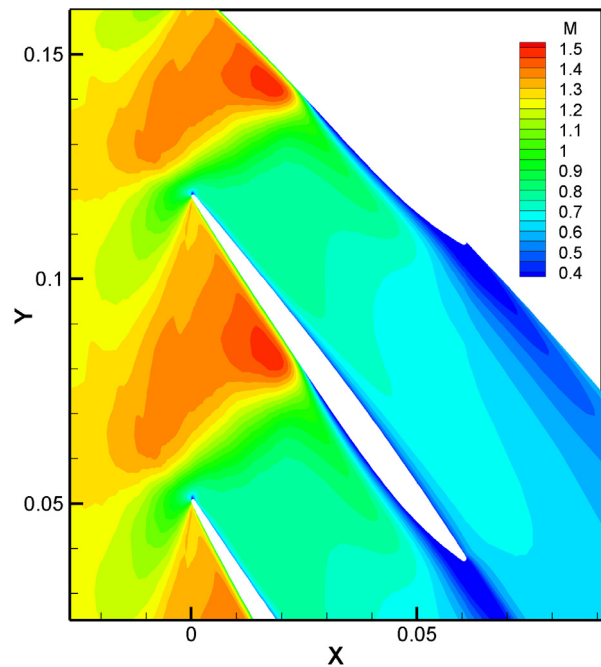**figure 10: Isentropic Mach number contours for DATUM blade at ∏=100%**

figure 11: Isentropic Mach number contours for DATUM blade at ∏=114%

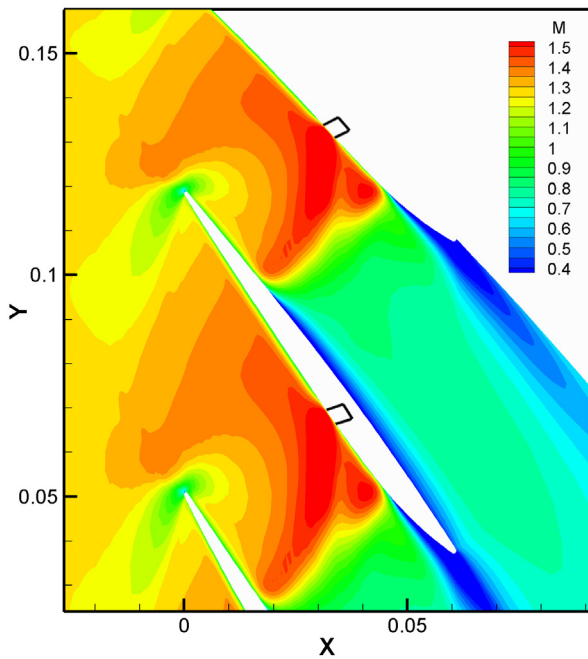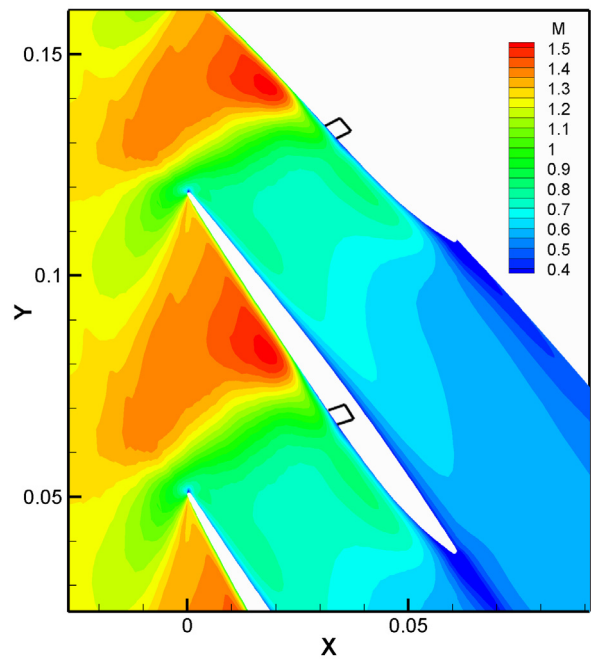**figure 12: Isentropic Mach number contours for ∏=100%, suction at 53% chord**

figure 14: Isentropic Mach number contours for ∏=123%, suction at 53% chord

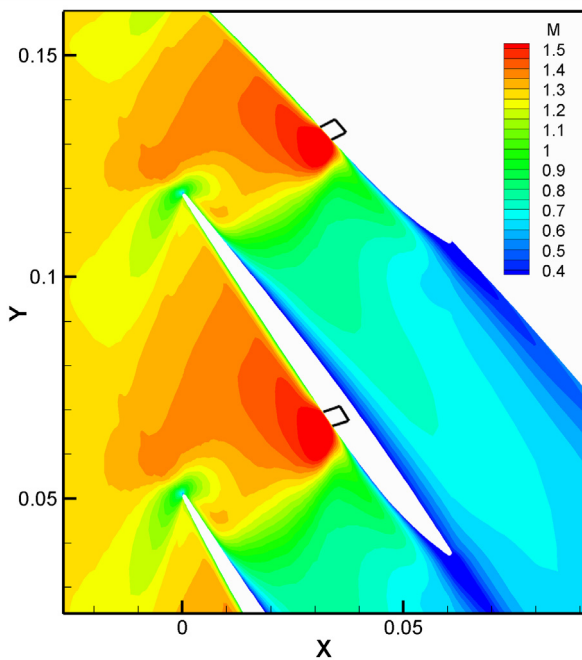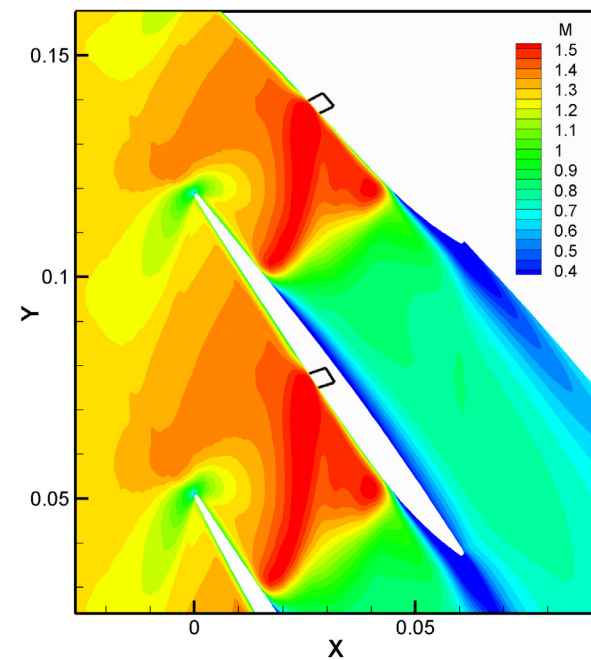**figure 13: Isentropic Mach number contours for ∏=114%, suction at 53% chord**

figure 15: Isentropic Mach number contours for ∏=100%, suction at 44% chord

In figure 14 the Mach number contours for the 53% suction close to stall is shown. First, it has to be noted that the flow stalls with BLS at a 10% higher pressure ratio, which is here 123% of design pressure ratio, when compared to the non-aspirated configuration. Second, the flow field looks very similar to the DATUM case at the limit to stall. The separation of the BL is aspirated away. The BLS removes the BL and at the same time decreases locally the pressure at the SS surface.

In figure 15 the Mach number contour of the 44% suction case is shown for the design pressure ratio. The flow field looks very similar to the 53% suction case, except of the interaction between the expansion wave and the shock. The location of the interaction between expansion/ recompression connected to the suction location and the passage shock is shifted from the normal shock wave to the PS surface. Additionally, the BL on the PS is accelerated and hence thinned by the expansion,

6

which impinges on the PS and is reflected as expansion on the solid wall.

In figure 16 the Mach number contour for the 43% suction is shown for the case with 123% of design pressure ratio. Here the shock foot bends locally to the suction location. It can be noted, that both suction locations prevent the shock from moving too much upstream, which would result in stall of the flow.
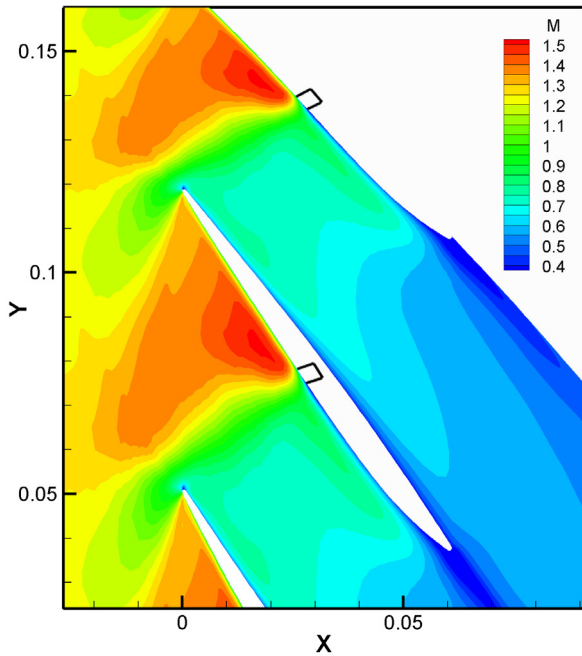

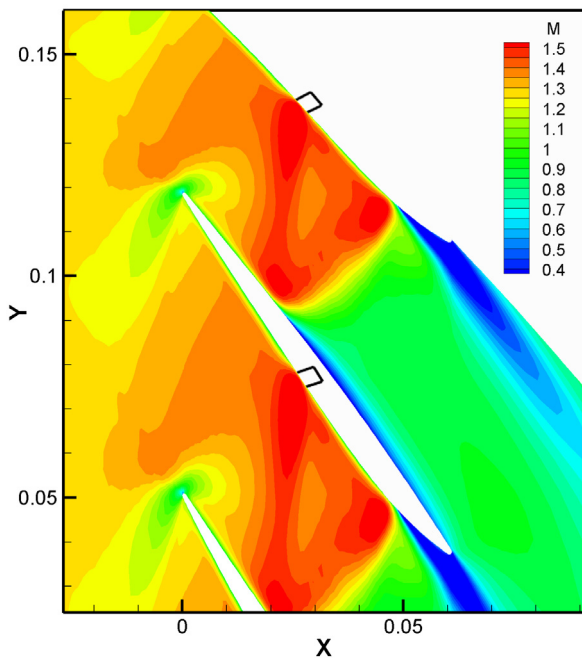**figure 16: Isentropic Mach number contours for ∏=123%, suction at 44% chord**

figure 17: Isentropic Mach number contours for ∏=87.6%, suction at 44% chord

In figure 17 the 44% suction case is shown for a lower backpressure, resulting in a pressure rise of 87.6% of design pressure ratio. This is of particular interest in order to study the effect of the expansion travelling to the PS, for a configuration where the normal passage shock is located more downstream than for the DATUM case at design conditions. The most important feature is a very high pre-shock Mach number on the SS and on the PS. The effect of the expansion, which travels through the whole passage and hits the flow on the PS and accelerates the BL on the PS is even more pronounced as in the cases with higher backpressure values. This higher pre-shock Mach number on the SS and PS is likely to produce a stronger shock with higher associated losses. This topic will be more thoroughly addressed in the discussion of the compressor performance map.

In figure 18 the computed compressor performance map is shown for one speed-line, in table 3 the mass flow, pressure ratio, isentropic efficiency and diffusion factor are given for the most important configurations. As the same boundary conditions (p_{t1}, T_{t1}, p_{s2}) are applied for the computations, the total pressure ratio is identical for the DATUM and the corresponding suction configurations.

One symbol represents one computation in figure 18, for the DATUM case 8 computations were carried out, whereas for the BLS cases results were obtained for higher pressure ratios resulting in 10 computations and thus symbols. For the lowest outlet pressure giving a pressure ratio of 87.6% of the design pressure ratio the mass flow rate is almost identical at 99% for the 3 configurations. The mass flow rate is increased at the design point by 1% for suction configuration 2. This increase in mass flow can be attributed to the fact that suction 2 is located at the nominal smallest throat area, where the suction increases the effective throat area by removing the BL. At an increased pressure ratio of 110% of design pressure the efficiency of the 2 suction configurations is equal to the DATUM case efficiency, and goes to peak efficiency for higher pressure ratios. For this higher pressure-ratio, the DATUM case computation does not give any valuable result, indicating that the flow stalls in the DATUM rotor. The higher efficiency values at higher pressure ratios can be attributed to the fact, that the shock remains in the passage even for this increased backpressure and thus the inlet flow angle remains optimum at the unique incidence condition.

There is a 2% reduction in isentropic efficiency for the suction configurations on the choked side of the characteristic when compared to the DATUM case. This surprising finding can be attributed to the fact that the BLS is located in the supersonic flow region. Here the BLS removes the BL and thus the effective flow channel geometry is more divergent in comparison to the non-suction case, resulting in an additional acceleration of the flow. An accelerated flow has a higher pre-shock Mach number resulting in higher losses. A second effect is the emission of the expansion wave with immediately behind a compression wave, which interacts with the passage shock, and in the worst case at smallest pressure ratio travels through the whole channel and impinges on the PS. This creates there a considerable higher pre-shock Mach number. As the expansion and recompression effect is usually irreversible this already creates more losses.

Name	Mass Flow [%]	Eta isen [%]	Pt2/Pt1 [% of design]	D'
Nosuction	100	88	100	0.53
Nosuction HP4	95	91	114	0.63
Suction1	100	86	101	0.54
Suction1 HP4	100	92	115	0.63
Suction1 HP6	97	94	123	0.68
Suction2	100	87	100	0.54
Suction2 HP4	100	92	115	0.62
Suction2 HP6	94	92	123	0.69

table 3: Computed efficiency, pressure ratio and diffusion for DATUM blade and suction configurations
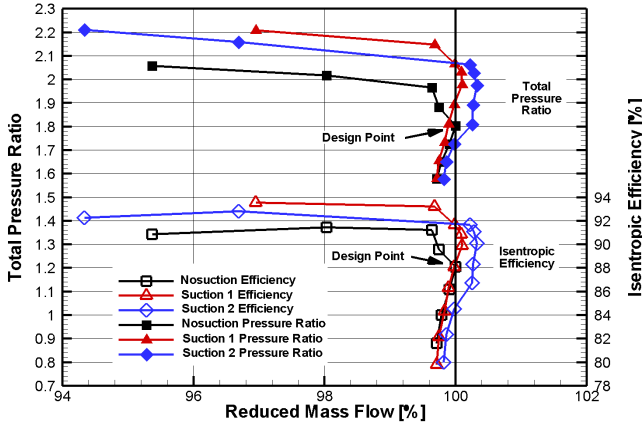

figure 18: Computed (Multip99a) compressor map without and with 2 different BLS locations for 100% of speed for reduced mass flow as fraction of design mass flow

The diffusion factor is used to assess the blade loading and is defined as follows (Cumpsty 1989):

$$D = 1 - \frac{c_2}{c_1} + \frac{\Delta c_u}{2 c_1 \frac{s'}{t'}} \leq 0.60 \qquad \text{eq. (2)}$$

The limit of 0.60 is considered being the limit where stall occurs, so a common value of 0.45 is likely to be taken for the design point (Cumpsty 1989). As shown in table 3 the diffusion factor of the DATUM case is 0.53, thus over the classical design goal of 0.45. The diffusion factor for the case on the onset of stall is 0.63 and so slightly above the stall limit. The diffusion for the cases with BLS shows for the same pressure ratio as for the stall case of the DATUM rotor a similar value of 0.63. A diffusion number of 0.68 and 0.69 is obtained for the onset of stall, thus almost 10% higher than the non-suction case. An increase of the same range has been obtained for the maximum pressure ratio, which augmented approximately by 10% for the cases with suction.

EXPERIMENTAL RESULTS

As the main purpose of the experimental campaign was so far to verify the reliability of the numerical design, the first step of the experiment was to obtain suitable inlet conditions at the test-section. In figure 19 the inlet Mach number and flow angle are shown over the channel height. As the channel height is limited to 40mm, it is desirable to obtain a constant inlet Mach number and inlet-angle, this is true from 20-90% of channel

height. At 10% of channel height the Mach number is smaller than 1 and the flow angle is smaller than 60 degree, which is likely to be provoked by a corner stall on the hub of the blade. The uniform inlet flow conditions could only be obtained with massive boundary layer suction on the channel walls up- and downstream of the measurement section. As Schulz (1993) showed the machine similarity is still assured for the middle region of the channel, even with the boundary layer suction on the channel wall.
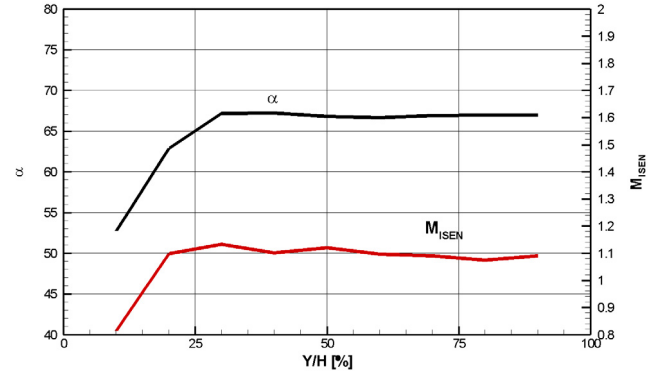

figure 19: Inlet flow angle and Mach number over the channel height

For the highest backpressure value for the DATUM case (114% of the design pressure) the isentropic surface Mach number evolution, measured via pressure taps, is shown in figure 20 in conjunction with the corresponding computations. The dots show the isentropic surface Mach number, the smooth solid line the computed isentropic surface Mach number.
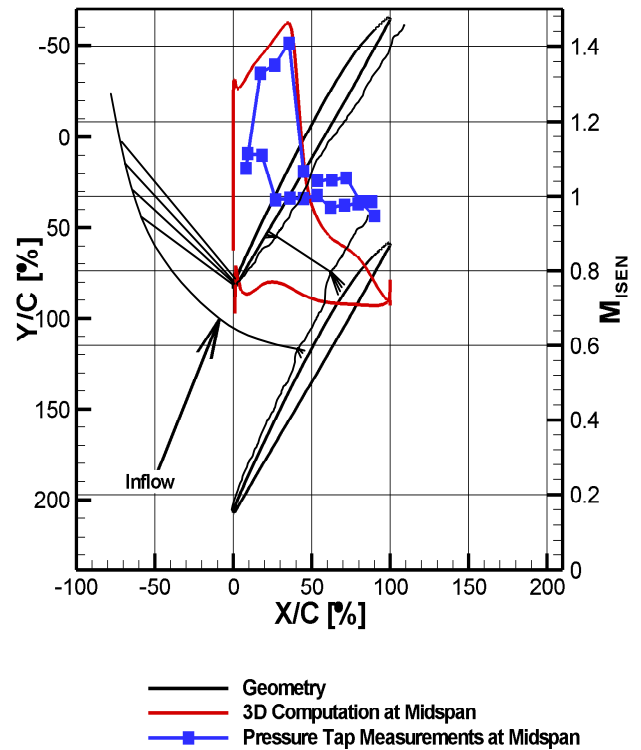

Geometry
3D Computation at Midspan
Pressure Tap Measurements at Midspan

figure 20: Isentropic surface Mach number, measured and computed – highest backpressure level, ∏=114%

The main shock location of the detached bow shock wave and the pre-shock Mach number on the SS of the blade is well predicted by the 3D computations. The measured inlet Mach number is smaller with a M_{inlet}=1.12 in comparison to M_{inlet}=1.2 for the computations. The difference in flow angle between the computations and the experiment is 2°: 67° and 65° for the experiment and the computation respectively. It is likely that these differences are created by the presence of the hub corner stall, which limits the maximum Mach number and flow rate. The main differences between the prediction and measurements are found for the flow on the PS. The prediction shows a completely subsonic flow on the PS, whereas the measurements do show up to 20% chord a supersonic flow and then behind a normal passage shock to almost subsonic flow conditions. As here the isentropic Mach number evolution is considered and the stagnation pressure is taken as reference at inlet, the flow might already be truly subsonic due to pressure losses, which are not captured when showing the isentropic surface Mach number. As it is sketched in figure 20, the measurements do suggest the presence of a detached bow shock wave and additionally the presence of a terminal passage shock, which was not captured by the 3D computations. The flat Mach number evolution behind the shock on the SS signals the presence of BL separation, which was not captured by the computations. This separation is in good agreement with the general limit for pre-shock Mach numbers of 1.3 for the separation limit. As the pre-shock Mach number is 1.4 separation would be expected

A higher backpressure, with a more frontward shock position could not be obtained in the test-rig. Any increase in backpressure resulted in the stall of the flow, which was indicated by the bow shock wave travelling to the pre-swirl vanes and thus unstarting the cascade.

CONCLUSIONS

A numerical study of a compressor rotor without and with boundary layer suction (BLS) has been performed with emphasis on the compressor working range. The relative inlet Mach number at mid-span is M_{inlet}=1.2. The computations cover one speed-line for varying back-pressure levels from choke to stall. Three different configurations are studied, DATUM rotor, 2 rotors with 2% suction mass flow, suction 1 at 53% and suction 2 at 44% of chord. The main result of the computations is that a suction mass flow of 2% design mass flow gave a 10% increase in pressure ratio and diffusion to D=0.69. The increase in working range could be used to shift the operating point of the compressor to a higher pressure-ratio and maintain the same stall margin as for the DATUM rotor. The case with the suction at 44% of chord does show a higher choking mass flow due to opening of the effective throat area, which would allow for a higher compressor mass flow.

As drawback of BLS the computations show a performance degradation for the BLS configurations, where the shock is located downstream of the suction location, which is usually the case at choked conditions. This performance penalty, which can attain 2% of isentropic efficiency, is likely to be created by the thinner BL aft the suction, provoking an acceleration of the flow in the more divergent flow channel. Additionally an expansion wave is emitted by the suction, which travels through the passage and impinges on the PS, thus accelerating the flow on the PS. This creates a higher pre-shock

Mach number on SS and PS and thus a stronger shock with higher associated losses.

Pressure tap measurements on the rotor with a supersonic relative inlet Mach number were carried out in LTT's annular cascade for the DATUM rotor. Here the inlet Mach number, inlet angle and isentropic surface Mach number distribution are shown for the operation point on the stall limit. Uniform inlet conditions could be obtained, which are crucial for such a prismatic rotor, which is aimed at the study of 2D flow in the channel middle. The agreement for the stall limit, shock location, pre-shock Mach number, inlet Mach number and angle between design and measurement is reasonable. The main difference is the presence of a channel shock in the measurement, which was absolutely not shown by the computations and a measured separation, which was not predicted by the computations.

FUTURE WORK

It would evidently be interesting to compare the computations with BLS to the corresponding measurements. Therefore it is planed to manufacture a second rotor incorporating slot suction on the SS in order to study experimentally the influence of BLS on the compressor characteristic. Furthermore it is planned to measure the total pressure loss over the DATUM rotor and the aspiration rotor with several aspiration rates in order to identify the true benefits of BLS in terms of losses.

REFERENCES

Bölcs, A,; 1993; *Turbomachines Thermiques Volume I,* Ecole Polytechnique Fédérale de Lausanne, Laboratoire de Turbomachines et de Thermique Appliquée

Bölcs, A., Suter, P.; 1986; *Transsonische Turbomaschinen,* Wissenschaft und Technik, Verlag G. Braun Karlsruhe, ISBN 3-7650-2036-2

Bölcs, A.; Hubrich, K.; Doerffer, P.; 2003; *Shock Wave - Boundary Layer Interaction Control by Stream-Wise Vortices*; Presented at the EFMC 2003, Toulouse, France

Cumpsty, N.A., 1989; *Compressor Aerodynamics,* Longman Scientific & Technical, ISBN 0-470-21334-5

Chaluvadi, V.S.P., Kalfas, A.I., Hodson, H.P, Ophyama, H., Wantanabe, E., 2002; *Blade Row Interaction in a High Pressure Steam Turbine,* ASME GT-2002-30574, Amsterdam, The Netherlands

Denton, J.D., 1999; *Multistage Turbomachinery Flow Calculation Program (MULTIP99) – User's Manual, Whittle Laboratory, University of Cambridge, April 1999*

Denton, J.D, Xu, L.; 2002 *The Effects of Lean and Sweep on Transonic Fan Performance,* ASME GT-2002-30327, Amsterdam, The Netherlands

Gregory-Smith, D.G., Crossland, S.D., 2001; *Prediction of Turbomachinery Flow Physics – Review of Recent Computations of APPACET Test Cases,* Task Quarterly 5 (ISSN 1428-6394), No. 4, 407-432, Lucerne May 2002

Dang, T.Q., van Rooij, M.P.C., Larosiliere, L.M., 2003; *Design of Aspirated Compressor Blades using Three-Dimensional Inverse Method,* ASME GT-2003-38492, Atlanta, Georgia

Hubrich, K., Bölcs, A.; 2004; *Study of the Modification of the Shock-Boundary Layer Interaction on an Isolated Airfoil by Slot Suction;* Paper accepted for publication on ISROMAC10, Honolulu 07-11. March 2004

Hubrich, K..;2004; *Measurements on an Isolated Blade with Boundary Layer Suction in the Laval Nozzle – Final Report;* Internal Report EPFL-LTT

Kerrebrock, J.L., Reijnen, D.P., Ziminsky, W.S, Smiig, L.M., 1997; *Aspirated Compressors,* ASME 97-GT-525, Orlando, Fl

Kerrebrock, J.L., Drela, M., Merchant, A.A., Schuler, B.J, 1998; *A Family of Designs for Aspirated Compressors,* ASMF 98-GT-196, Stockholm, Sweden

Lord, W.K.; MacMartin, D.G.; Tillman, T.G.; *Flow Control Opportunities in Gas Turbine Engines,* Fluids 2000**,** AIAA June 2000 in Denver, AIAA 2000-2234

Merchant, A.A., 1999 ; *Design and Analysis of Axial Aspirated Compressor Stages,* PhD Thesis June 1999 MIT

Rottmeier, F.; 2003; *Experimental Investigation of a Vibrating Axial Turbine Cascade in Presence of Upstream Generated Aerodynamic Gusts,* PhD Thesis 2758 Ecole Polytechnique Fédérale de Lausanne

Schulz, K., 1993; *Experimentelle Untersuchung der Verlustmechanismen und Arbeitsgrenzen von transsonischen Verdichtergittern,* PhD Thesis 1122 Ecole Polytechnique Fédérale de Lausanne